

## Effect of a Chain Extender on the Rheological and Mechanical Properties of Biodegradable Poly(lactic acid)/Poly[(butylene succinate)-*co*-adipate] Blends

Hassan Eslami, Musa R. Kamal

Department of Chemical Engineering, McGill University, 3610 University Street, Montreal, Quebec H3A 2B2, Canada  
Correspondence to: M. R. Kamal (E-mail: musa.kamal@mcgill.ca)

**ABSTRACT:** Biodegradable polymer blends based on poly(lactic acid) (PLA) and poly[(butylene succinate)-*co*-adipate] (PBSA) were prepared with a laboratory internal mixer. An epoxy-based, multifunctional chain extender was used to enhance the melt strength of the blends. The morphology of the blends was observed with field emission scanning electron microscopy. The elongational viscosities of the blends, with and without chain extender, were measured with a Sentmanat extensional rheometer universal testing platform. The blends with chain extender exhibited strong strain-hardening behavior, whereas the blends without chain extender exhibited only weak strain-hardening behavior. Measurements of the linear viscoelastic properties of the melts suggested that the chain extender promoted the development of chain branching. The results show that PBSA contributed to significant improvements in the ductility of the PLA/PBSA blends, whereas the chain extender did not have a significant effect on the elastic modulus and strain at break of the blends. The combined blending of PLA with PBSA and the incorporation of the chain extender imparted both ductility and melt strength to the system. Thus, such an approach yields a system with enhanced performance and processability. © 2013 Wiley Periodicals, Inc. *J. Appl. Polym. Sci.* 129: 2418–2428, 2013

**KEYWORDS:** biodegradable; blends; mechanical properties; rheology

Received 5 May 2012; accepted 9 August 2012; published online 30 January 2013

**DOI:** 10.1002/app.38449

### INTRODUCTION

The main source of the thermoplastic polymers used currently in the packaging industry is nonrenewable crude oil and natural gas. Even though many techniques are used to recycle and reuse these materials, a large part of them is disposed in landfills or incinerators; this leads to environmental and waste-management problems. Replacing petroleum-based plastics with biodegradable and compostable polymers derived from renewable sources is highly desirable from both an economic and environmental standpoint. Biodegradable polymers are generally environmentally friendly, with little or no harmful impact on landfills.

Among many biodegradable polymers, poly(lactic acid) (PLA) has attracted considerable attention because of its excellent gloss and clarity, high tensile strength, good heat sealability, and low coefficient of friction. These properties make PLA a suitable candidate for a wide variety of packaging applications.<sup>1</sup> However, drawbacks, including a low melt strength and brittleness, limit its end-use applications. The blending of PLA with other biodegradable polymers, such as poly[(butylene succinate)-*co*-adipate] (PBSA) and poly[(butylene adipate)-*co*-(butylene terephthalate)] (PBAT) presents a potential approach to

overcoming the aforementioned limitations. Along these lines, Jiang et al.<sup>2</sup> studied the mechanical properties of PLA/PBAT blends at various blend compositions. They reported that the elongation at break and toughness of these blends were significantly better than those of PLA, even at low concentrations of PBAT. Tensile tests and scanning electron microscopic images of the blends showed that the failure mode changed from brittle fracture for pure PLA to ductile fracture for the blends. Eslami and Kamal<sup>3</sup> evaluated the elongational rheology of PLA/PBSA blends with different blend compositions. They found that PLA/PBSA blends containing less than 50 wt % PBSA showed no clear strain-hardening behavior. However, a well-defined strain-hardening behavior was observed for blends containing PBSA at concentrations of 50 wt % or higher. Thus, the melt strength of the blend was improved only when PBSA formed a continuous phase in the blend, which usually occurred at high content of PBSA. They also reported that the ductility of the blends improved significantly, even at low concentrations of PBSA.<sup>4</sup>

Another strategy for enhancing the melt strength of PLA is the creation of a branched architecture with chain-extension reactions.<sup>5–7</sup> Along these lines, Corre et al.<sup>5</sup> investigated the effects

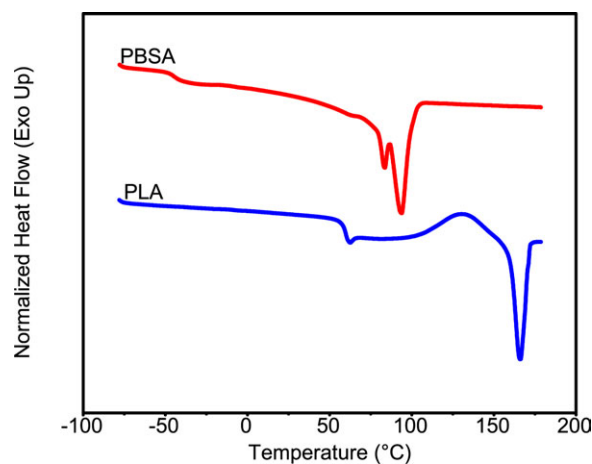


**Figure 1.** DSC thermograms of pure PLA and PBSA. [Color figure can be viewed in the online issue, which is available at [wileyonlinelibrary.com](http://wileyonlinelibrary.com).]

of an epoxy-functionalized chain extender on the rheological behavior of PLA. They reported that the chain extender modified the molecular structure of PLA considerably by adding a high-molecular-weight shoulder to the molecular weight distribution of PLA. They found that the melt rheology of PLA with the chain extender was improved in both shear and extensional flows. However, they reported that some processing limitations arose at a very high extension ratio (a high content of chain extender) because of the high melt elasticity. Li and Huneault<sup>6</sup> studied the effects of the chain-extension reaction on the properties of PLA/thermoplastic starch (TPS) blends. They used a multifunctional, epoxy-based chain extender to improve the rheological and end-use properties of the blends. They found that the carboxyl end groups of PLA could potentially react with the epoxy groups in the chain extender, and this led to an increase in the molecular weight through the chain-extension reaction. Moreover, the presence of multifunctional reaction sites in the chain extender increased the chance for the formation of a branched structure in PLA.<sup>6</sup> In another study, Mihai et al.<sup>7</sup> investigated the rheology and extrusion foaming of PLA. They used an epoxy-based chain extender to modify the melt rheology, particularly, the elongational rheology, of PLA. They prepared PLA with various contents of chain extender and measured the shear and elongational flow properties. They found that the viscosity and elasticity of PLA increased as the concentration of chain extender increased. Moreover, the elongational flow properties (e.g., strain-hardening behavior) of PLA improved dramatically in the presence of the chain extender. The strain-hardening behavior became stronger as the concentration of chain extender increased. The chain-branched architecture of PLA was assumed to be responsible for the high melt strength, high zero-shear viscosity, high elasticity, and enhanced shear-thinning behavior.<sup>7</sup>

Although a considerable amount of work has been devoted to biodegradable polymer blends,<sup>8–12</sup> little attention has been paid to biodegradable polymer blends based on PLA and PBSA. Therefore, the objective of this study was to prepare biodegradable PLA/PBSA blends with and without chain extender and to

investigate their morphological, mechanical, and rheological properties, with special emphasis on their elongational rheology.

## EXPERIMENTAL

### Materials

The PLA used in this study was supplied by NatureWorks, LLC, Blair, Nebraska, USA, and had the designation 7032D. It is recommended for stretch blow molding for potential application in bottles. PLA is synthesized by the ring-opening polymerization of lactides or the condensation polymerization of lactic acid monomers.<sup>13</sup> Synthetic biodegradable PBSA (Bionolle 3001 M) was obtained from Showa High Polymer, Ltd. (Shanghai, Japan). According to the supplier, the PBSA had a mass density of 1230 kg/m<sup>3</sup>. PBSA is a random copolyester synthesized by the polycondensation of 1,4-butanediol in the presence of succinic and adipic acids. It contains highly flexible macromolecules with an excellent impact strength. The mechanical properties and processability of PBSA are comparable to those of polyolefins.<sup>14</sup> The thermal behavior of the net PLA and PBSA, obtained from differential scanning calorimetry at a rate of 5°C/min, is shown in Figure 1. The main thermal characteristics of PLA and PBSA are presented in Table I. Two distinct melting points were observed for PBSA, whereas a single melting point was observed for PLA. Moreover, a cold crystallization temperature was observed for PLA. A multifunctional chain extender [CESA Extend OMAN698493 (CESA)] was used as a chain extender. It is an additive based on epoxy-functionalized PLA. It was supplied by Clariant Masterbatches. According to the supplier, CESA is a masterbatch based, Muttez, Switzerland on a molecule originally developed to relink polymer chains in degraded condensation polymers. Recently, it was shown that CESA can significantly improve the melt strength of PLA.<sup>5</sup>

### Preparation of the Blend

All of the materials were dried *in vacuo* at 55°C for a period of 48 h before processing. Mixing was carried out with an internal mixer (Thermo Haake Mixer, Waltham, MA, USA) with a mixing volume of 60 cm<sup>3</sup> and equipped with three controllable heating zones. PLA with chain extender and blends of PLA and PBSA with and without chain extender were prepared at a single composition of 70/30 PLA/PBSA (see Table II for more detail). For blends without chain extender, granules of PLA and PBSA were first hand-mixed in a plastic container. The hand-mixed samples were then fed into the internal mixer. For blends with chain extender, the chain extender, also in the form of pellets, was added to the blend in the melt state. Blends with chain extender were prepared at a single CESA concentration (2 wt %). All mixing was performed at 180°C and a rotor speed of 60 rpm under a nitrogen atmosphere. Mixing was carried out for

**Table I.** Thermal Characteristics of the Pure Components

Resin	Glass-transition temperature (°C)	Cold crystallization temperature (°C)	Melting point 1 (°C)	Melting point 2 (°C)
PLA	59	130	165	—
PBSA	-44	—	83	94

**Table II.** Compositions of the PLA/PBSA Blends with and without Chain Extender

PLA (wt %)	PBSA (wt %)	CESA (wt %)	Mixing time (min)	Nomenclature
98	0	2	5	PLA2CESA5min
98	0	2	10	PLA2CESA10min
98	0	2	15	PLA2CESA15min
98	0	2	20	PLA2CESA20min
70	30	0	5	PLA30PBSA5min
70	30	0	20	PLA30PBSA20min
70	30	2	5	PLA30PBSA2CESA5min
70	30	2	20	PLA30PBSA2CESA20min

different mixing times (5, 10, 15, and 20 min). Pure PLA and chain extender (2 wt %) were also mixed under the same processing conditions. Hereafter, the PLA with chain extender (PLA2CESA5min and PLA2CESA20min) and the PLA/PBSA blends with chain extender (PLA30PBSA2CESA5min and PLA30PBSA2CESA20min) are referred to as compounds with chain extender. To prevent any possible degradation and also to freeze the morphology of the blends, the samples were quickly cooled in liquid nitrogen after processing. Pure PLA and PBSA were processed under the same processing conditions described previously.

### Morphological Characterization

The samples for scanning electron microscopy (SEM) were prepared by the cryofracturing in liquid nitrogen of the samples obtained from the internal mixer. The cryofractured samples were then coated with gold–palladium vapor deposition for a period of 30 s. The morphology of the blends was observed by field emission scanning electron microscopy (FE-SEM; Hitachi S-4700, Tokyo, Japan, operated at 2 kV).

### Rheological Measurements

Small-amplitude oscillatory shear (SAOS) measurements were performed with a stress-controlled rheometer (Physica MCR 501, Anton Paar, Graz, Austria) with parallel-plate configuration at 180°C. A disk-shaped specimen (25 mm in diameter and 1.5 mm in thickness) was first placed in the parallel-plate fixture and left to rest for 10 min. We then adjusted the gap to 1 mm by squeezing the sample. Dynamic frequency ( $\omega$ ) sweep experiments were then performed in the linear viscoelastic region over a range of  $\omega$  from 0.1 to 100 rad/s. Disk-shaped specimens were prepared with a Carver press (Wabash, IN, USA) operated at 5 MPa and 180°C for a period of 10 min (4 min of preheating, 3 min of heating under pressure, and 3 min of cooling under pressure).

The elongational viscosity was measured with a Sentmanat extensional rheometer (SER) universal testing platform (Xpansion Instruments, LLC, Tallmadge, OH, USA) in combination with the Anton Paar Physica MCR 501 rotational rheometer. Transient stress-growth experiments were carried out over a range of Hencky strain rates from 0.5 to 8 s<sup>-1</sup>. The test temperature was kept at 180°C. The detailed operating principle of the SER uni-

versal testing platform can be found elsewhere.<sup>15,16</sup> To prepare the specimens for testing, the samples obtained from the internal mixer were molded into rectangular sheets (with a nominal thickness of 0.5 mm) in the Carver press with a flat window frame mold. Compression molding was carried out at 5 MPa and 180°C for a period of 10 min, as described previously. A dual-blade cutter with a fixed-gap spacer was then used to cut a rectangular specimen with a fixed width. The ultimate approximate dimensions of the test specimen were a length of 17 mm, a width of 12.7 mm, and a thickness of 0.5–0.6 mm. It is worth mentioning that the loading procedure of the sample (i.e., opening the door of the oven chamber, fixing the sample onto the SER fixture, and finally closing the door of the oven chamber) and the waiting period before starting the test have a substantial influence on the accuracy and reproducibility of the extensional experiment. More specifically, the sample has to be loaded in the fixture as fast as possible to minimize the temperature drop of the oven chamber. Furthermore, to prevent sagging of the sample, the test has to be started as soon as the sample reaches its equilibrium temperature. In this study, the loading procedure took about 30 s, and the sample was allowed to reach its equilibrium temperature for a period of about 2 min.

### Tensile Testing

The dumbbell-shaped specimens for tensile testing (according to ASTM D 638) were prepared with a Carver press operated at 5 MPa and 180°C for a period of 10 min, as described previously. The tensile tests were conducted with an MTS universal tensile testing machine (Eden Prairie, MN, USA). A crosshead speed of 5 mm/min was used for all tests.

## RESULTS AND DISCUSSION

### Morphology

Figure 2(a,b) shows the FE-SEM images of the fractured surfaces of the PLA/PBSA blends without chain extender prepared for mixing times of 5 and 20 min, respectively. The results indicate that the dispersed phase, PBSA, exhibited a droplet morphology with small mean diameters. A comparison between Figures 2(a) and 2(b) showed that the mixing time had no significant effect on the size of the droplet domain. However, when the mixing time was increased, the droplets become more uniform. Figure 3(a,b) presents the FE-SEM images of the fractured surfaces of the PLA/PBSA blends with chain extender, prepared with mixing times of 5 and 20 min, respectively. These figures show that an increase in the mixing time changed the morphology from a droplet morphology to a nearly cocontinuous morphology. The results of SEM analyses indicate that the incorporation of chain extender reduced the scale of morphological features compared to the corresponding blends without chain extender. In particular, for blends that exhibited droplet morphology, the mean diameter of the droplets became smaller in the presence of chain extender [cf. Figure 2(a)–3(a)]. Moreover, the chain extender induced a change in the morphology from droplet to nearly cocontinuous when blending took place for longer mixing times [cf. Figure 2(b)–3(b)].

### Rheology

**Transient Elongational Flow.** Elongational viscosity data for pure PLA and pure PBSA at various elongational rates are presented in Figure 4(a,b), respectively. Transient elongational tests

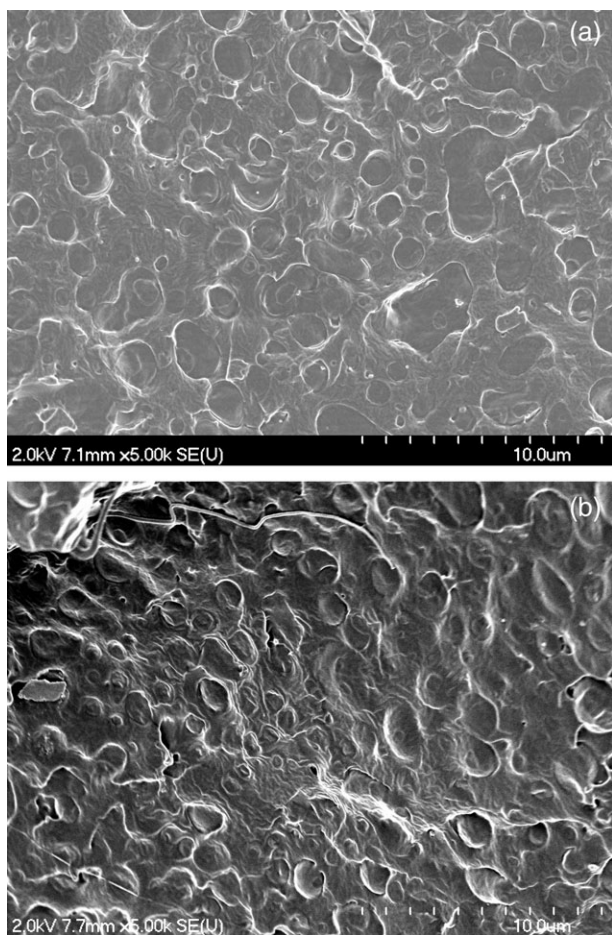


**Figure 2.** FE-SEM images of the PLA/PBSA blends at mixing times of (a) 5 and (b) 20 min.

were performed at strain rates of greater than  $0.5 \text{ s}^{-1}$ , where a reproducible signal could be obtained from the rheometer for all samples. As shown in Figure 4(a), the elongational viscosity of pure PLA showed no strain-hardening behavior over the entire range of applied strain rates. The linear chain structure of PLA was likely to be responsible for its strain-softening behavior under transient uniaxial extensional flow. The results of the elongational test for pure PBSA, on the other hand, show strong strain-hardening behavior at a strain rates as low as  $0.5 \text{ s}^{-1}$ .

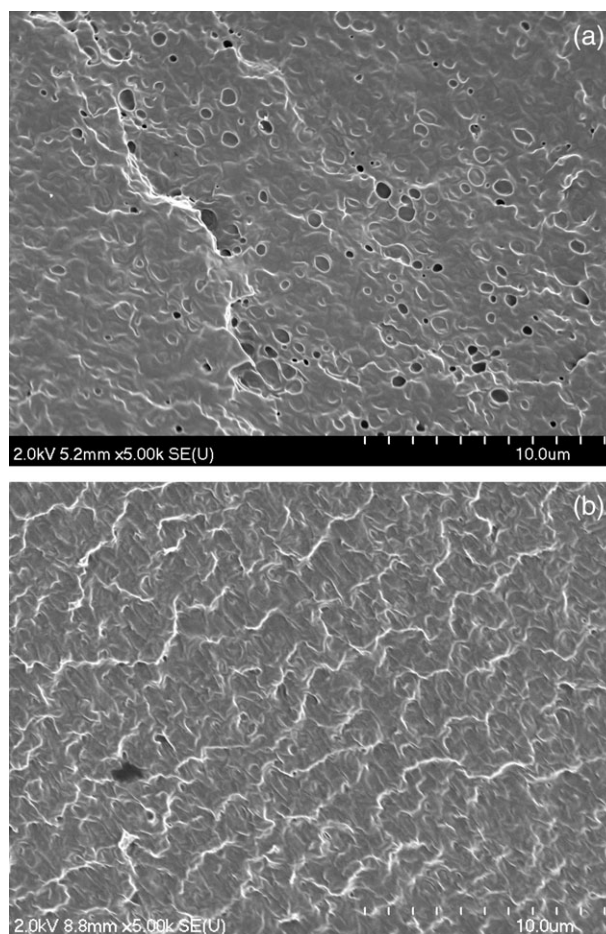
The results of the transient elongational viscosity for the PLA/PBSA blends without chain extender prepared at two different mixing times are shown in Figure 5. Figure 5(a) shows the very weak strain-hardening behavior for the PLA/PBSA blends prepared with a 5-min mixing time. With increasing mixing time [see Figure 5(b)], no significant improvement was observed in the strain-hardening behavior of the PLA/PBSA blends. However, with increasing mixing time, the data of the transient elongational tests became less noisy, which could have been an indication of a more uniformly mixed blend. The more uniform droplet morphology observed for the PLA/PBSA blends prepared at high mixing times supported this explanation [see Figure 2(a,b)].

Four different mixing times were used to investigate the effect of the mixing time on the elongational flow behavior of PLA

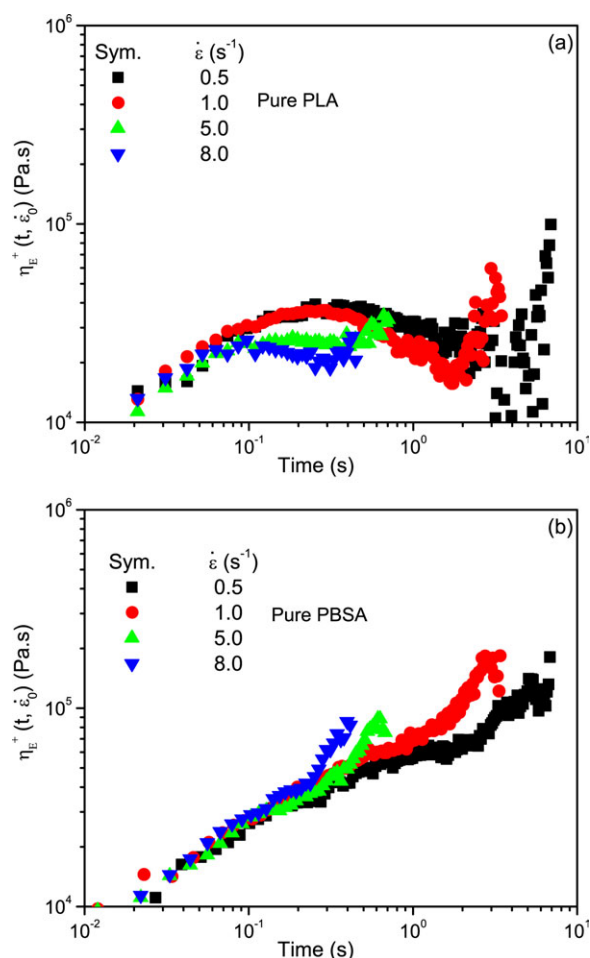
with chain extender. The results of the elongational flow experiments for compounds of PLA with chain extender (PLA2CESA) prepared at various mixing times are presented in Figures 6(a–d). At low mixing time (i.e., for the compound prepared with 5 min of mixing), no strain-hardening behavior was observed in the entire range of applied strain rates [Figure 6(a)]. As the mixing time increased, the compound started to show noticeable strain-hardening behavior. For the compound prepared with 20 min of mixing, a well-defined strain-hardening behavior was observed [see Figure 6(d)]. The strain-hardening behavior of PLA with chain extender was possibly due to the chain-branched structure of PLA formed as a result of the chain-extension reaction. The intensity of the chain-branched structure increased as the mixing time increased.

Figure 7(a,b) presents the elongational viscosity of the PLA/PBSA blends with chain extender prepared with 5- and 20-min mixing times, respectively. We observed that the incorporation of CESA into the PLA/PBSA blends imparted strain-hardening behavior to the blends. The blends exhibited well-defined strain-hardening behavior, which became stronger as the mixing time was increased.

The effect of the chain extender on the uniaxial elongational viscosity at a strain rate of  $5 \text{ s}^{-1}$  is shown in Figure 8(a,b) for



**Figure 3.** FE-SEM images of the PLA/PBSA/CESA blends at mixing times of (a) 5 and (b) 20 min.



**Figure 4.** Elongational viscosity values of the (a) pure PLA and (b) pure PBSA at various strain rates. [Color figure can be viewed in the online issue, which is available at [wileyonlinelibrary.com](http://wileyonlinelibrary.com).]

compounds prepared with 5- and 20-min mixing times, respectively. As shown in Figure 8(a), the elongational viscosity of the pure PLA and PLA/PBSA blend without chain extender increased monotonically with time and then leveled off. However, the elongational viscosity of the pure PBSA abruptly increased with time. Figure 8(a) shows that the elongational viscosity of PLA with chain extender increased with time and then leveled off. However, its absolute value was higher than that of the pure PLA and PLA/PBSA blend without chain extender. The elongational viscosity of the PLA/PBSA blend with chain extender also increased with time. Its magnitude was higher than those of the pure PBSA and PLA/PBSA blend without chain extender. For compounds prepared with higher mixing times, the elongational viscosities of compounds with chain extender were higher than those of the pure components and blends without chain extender. This was possibly because at high mixing times, the chain-extension reaction was more advanced, and a more extensive chain-branched structure was obtained for compounds with chain extender. A comparison between Figures 8(a) and 8(b) revealed that the strain-hardening became more pronounced as the mixing time was increased, particularly for compounds with chain extender.

To observe the morphology of the blends after elongational tests, the samples were quickly cooled with compressed air and cryofractured in liquid nitrogen. Figure 9(a,b) presents the FE-SEM images of the PLA/PBSA blends with chain extender before and after elongational viscosity measurements, respectively. The results show that the droplets were elongated in the direction of stretching. The final morphology changed from a droplet morphology to an elongated droplet morphology.

**SAOS Flow.** Structural changes in polymeric systems can be evaluated with the linear viscoelastic properties obtained from SAOS experiments. In fact, SAOS measurements are very sensitive to the topological structure of macromolecular chains, as in long-chain branching. The results of SAOS measurements for the individual polymers and the blends with and without chain extender are presented in Figure 10. The complex viscosity ( $\eta^*$ ) data, presented in Figure 10(a), showed that the pure PLA exhibited a clear Newtonian plateau at low  $\omega$ ; this was followed by decreasing  $\eta^*$  at higher  $\omega$ s. However,  $\eta^*$  of pure PBSA did not show a Newtonian plateau, at least in the  $\omega$  range investigated in this study. At low  $\omega$ , the  $\eta^*$  of pure PBSA was higher

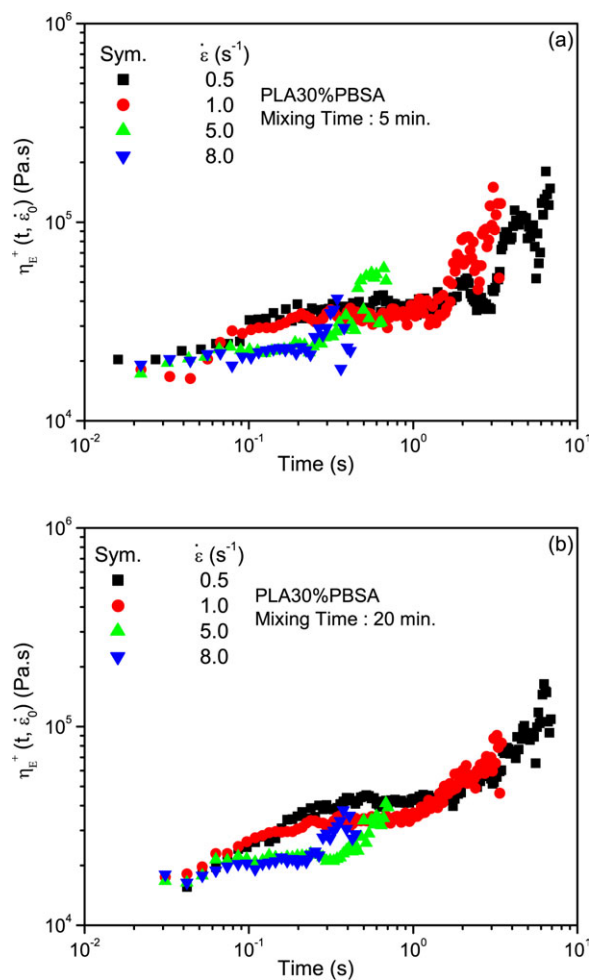


**Figure 5.** Elongational viscosity values of the PLA30%PBSA (PLA/PBSA:70/30) blends at various mixing times: (a) 5 and (b) 20 min. [Color figure can be viewed in the online issue, which is available at [wileyonlinelibrary.com](http://wileyonlinelibrary.com).]

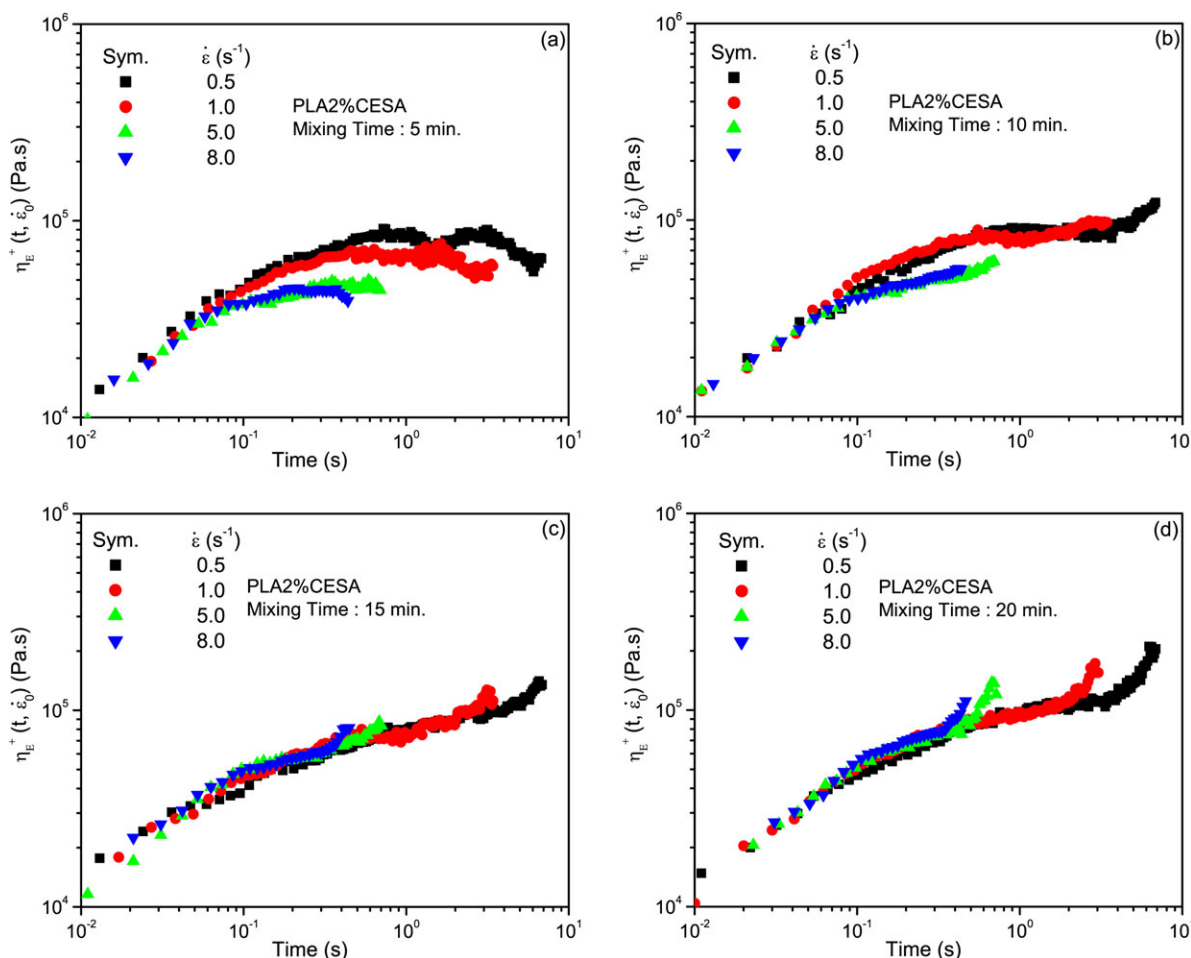


**Figure 6.** Elongational viscosity values of the PLA2%CESA (PLA/CESA: 98/2) blends at various mixing times: (a) 5, (b) 10, (c) 15, and (d) 20 min. [Color figure can be viewed in the online issue, which is available at [wileyonlinelibrary.com](http://wileyonlinelibrary.com).]

than that of pure PLA. At high  $\omega$ , on the other hand,  $\eta^*$  of pure PBSA became lower than that of pure PLA. Figure 10(a) indicates that at low  $\omega$ s, the  $\eta^*$  values of the blends without chain extender (PLA30PBSA5min and PLA30PBSA20min) were greater than that of pure PLA and that they increased slightly with increasing mixing time (i.e.,  $\eta^*$  of PLA30PBSA20min was higher than that of PLA30PBSA5min). At high  $\omega$ s, the  $\eta^*$  values of the blends without chain extender were between the  $\eta^*$  values of pure PLA and pure PBSA. On the other hand, the  $\eta^*$  values of the compounds with chain extender (PLA with chain extender and PLA/PBSA blends with chain extender, PLA2CESA5min, PLA2CESA20min, PLA30PBSA2CESA5min, and PLA30PBSA2CESA20min) were higher than those of the pure components in the entire range of  $\omega$ s. Moreover, no clear sign of a Newtonian plateau at low  $\omega$  was observed for compounds with chain extender, at least in the  $\omega$  range investigated in this study. These observations revealed the presence of a microstructure with a long relaxation time.

Figure 10(b) shows the storage modulus ( $G'$ ) of the pure components, blends without chain extender, and compounds with chain extender.  $G'$  of the blends without chain extender increased slightly with increasing mixing time. In the low- $\omega$  region,  $G'$  values of compounds with chain extender were

higher than those of the both pure PLA and blends without chain extender. Because  $G'$  is a measure of the elasticity of a system, this indicates that the elasticity of the compounds with chain extender was higher than that of the blends without chain extender. Moreover, the elasticity increased with increasing mixing time.

Figure 10(a) shows that  $\eta^*$  at low  $\omega$ s of compounds with chain extender was quite high compared to those of the same compounds without chain extender. In compounds with chain extender, the transition from a Newtonian plateau to the so-called shear-thinning regime shifted to very low  $\omega$ . These characteristics generally observed in the linear rheology of polymeric systems with a long-chain-branching structure.<sup>17,18</sup>  $G'$  is even more sensitive to the structural changes in viscoelastic materials. In the terminal region of polymeric materials with linear macromolecular chains,  $G'$  is proportional to the square of  $\omega$  (i.e.,  $G' \propto \omega^2$ ). The loss modulus ( $G''$ ) grows linearly with  $\omega$  (i.e.,  $G'' \propto \omega$ ).<sup>18</sup> The results presented in Figure 10(b) indicate that all of the samples, except pure PLA, deviated from the terminal behavior. The deviation became more pronounced for compounds with chain extender. More specifically, the slope of  $G'$  versus  $\omega$  decreased from 1.91 for pure PLA to 1.11 for PLA2CESA20min and to 0.67 for PLA30PBSA2CESA20min. This

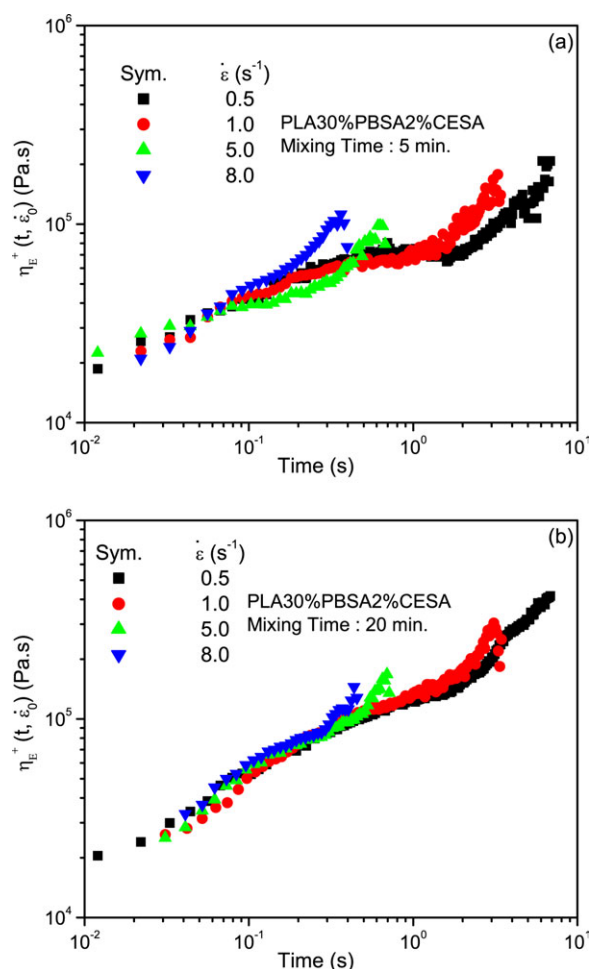


**Figure 7.** Elongational viscosity values of the PLA30%PBSA2%CESA (PLA30PBSA2CESA5min, PLA30PBSA2CESA20min) blends at two different mixing times: (a) 5 and (b) 20 min. [Color figure can be viewed in the online issue, which is available at [wileyonlinelibrary.com](http://wileyonlinelibrary.com).]

nonterminal behavior observed for compounds with chain extender could have been associated with a chain-branching structure, which led to a long terminal relaxation time. It is worth mentioning that in the case of the blends with chain extender, part of the deviation from terminal behavior could have been related to the structure and morphology of the blends.

The Cole–Cole plot (the curve of  $\eta''$ , out-of-phase component of complex viscosity vs  $\eta'$ , dynamic viscosity) is usually used to examine the structural changes in long-chain-branched macromolecules and multicomponent multiphase polymer systems. As shown in Figure 11(a), for pure PLA and PBSA, a concave Cole–Cole curve close to a semicircle is obtained. The Cole–Cole plots of the blends without chain extender deviated slightly from the semicircular shape and could be associated with the structure of the blend. However, the Cole–Cole plots of compounds with chain extender deviated significantly from the semicircular shape; this indicated a long relaxation time at low  $\omega$ s. The deviation from the semicircular shape was more obvious for blends with chain extender than for PLA with chain extender. This could have been associated with the morphology of the blends.

The Cole–Cole plot represents an empirical correlation between  $\eta''$  and  $\eta'$ . However, the modified Cole–Cole plot (the curve of  $\log G'$  vs  $\log G''$ ) at a fixed temperature has been used widely for the evaluation of structural changes in polymer blends and filled polymer systems.<sup>19–21</sup> The modified Cole–Cole plots for the pure components, blends without chain extender, and compounds with chain extender are presented in Figure 11(b). The results show that the modified Cole–Cole plots of the blends deviated from those of the pure components. The slopes of the  $\log G'$  versus  $\log G''$  plots for the blends were smaller to those for pure components. This suggests that all of the PLA/PBSA blends were immiscible and confirmed the results of the SEM observations.<sup>19</sup> A comparison between the modified Cole–Cole plots of the blends without chain extender and compounds with chain extender revealed that the deviation from the terminal relation (i.e.,  $G' \sim G''^2$  generally observed for linear polymers) became more pronounced in compounds with chain extender. Nonlinear behavior in the log–log scale was clearly observed in the modified Cole–Cole plot of the PLA/PBSA blends with chain extender. Moreover, the values of  $G'$  for the blends with

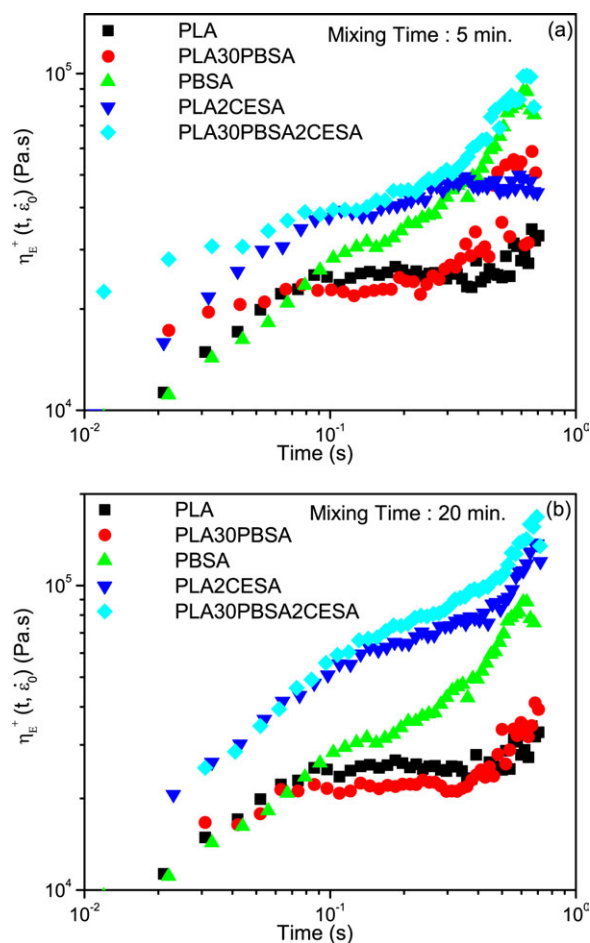


**Figure 8.** Comparison between the elongational viscosity values of various compounds of the PLA/PBSA blends (PLA30PBSA:PLA/PBSA:70/30, PLA2-CESA: PLA/CESA:98/2, PLA30PBSA2CESA:PLA/PBSA/CESA:70/30/2) at an elongational rate of  $5 \text{ s}^{-1}$  at mixing times of (a) 5 and (b) 20 min. [Color figure can be viewed in the online issue, which is available at [wileyonlinelibrary.com](http://wileyonlinelibrary.com).]

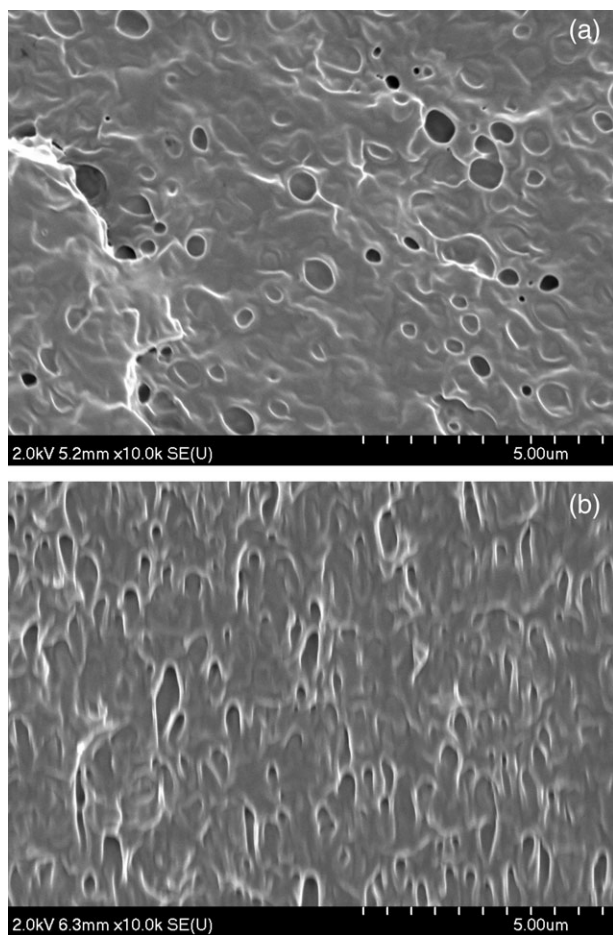


**Figure 9.** FE-SEM images of the PLA30%PBSA2%CESA blends (mixing time = 5 min) (a) before and (b) after the elongational viscosity test at an elongation rate of  $8 \text{ s}^{-1}$ .

chain extender were not only higher than those for the pure components but were also higher than those for the blends without chain extender. These observations reflected the additional structural changes in the blends containing chain extender that were due to the presence of chain branching.

The results of the SAOS experiments show that a longer relaxation process appeared in the compounds with chain extender compared to the corresponding compounds without chain extender. This longer relaxation process may have been due to the chain-branched structure formed in compounds with chain extender. Furthermore, an increase in the mixing time led to more extensive chain branching, which was reflected qualitatively in the results of SAOS experiments. Yu et al.<sup>18</sup> made similar observations and had similar conclusions in the case of long-chain-branched polypropylene. In the case of PLA, Corre et al.<sup>5</sup> used the same chain extender as we used in this study and concluded that the chain extender modified the molecular structure of PLA by adding a high-molecular-weight shoulder to the unimodal molecular weight distribution of PLA. Mihai et al.<sup>7</sup> also used the same chain extender for PLA and concluded that branching occurred through a chain-extension reaction.

### Mechanical Properties

The stress–strain curves of the blends and pure components are depicted in Figure 12. A clear yield point was observed for the pure PLA, followed by instant rupture. The same behavior was observed for PLA with chain extender (i.e., PLA2CESA5min and PLA2CESA20min). This is the typical behavior generally observed for brittle materials. On the other hand, the stress–strain curves for the blends, with and without chain extender, showed a noticeable yield stress followed by stable necking. As the strain increased, the neck grew until ductile failure occurred. Thus, the pure PLA and PLA with chain extender showed brittle fracture, whereas all of the blends showed ductile behavior.

The elastic modulus and strain at break of PLA with chain extender prepared with different mixing times, along with those of pure PLA, are presented in Figure 13(a,b), respectively. The results reveal that the chain extender had no significant effect on the previous mechanical properties of PLA. Moreover, the mixing time did not significantly change the elastic modulus and strain at break of PLA.

The elastic modulus and strain at break of the PLA/PBSA blends with and without chain extender, along with those of pure PLA

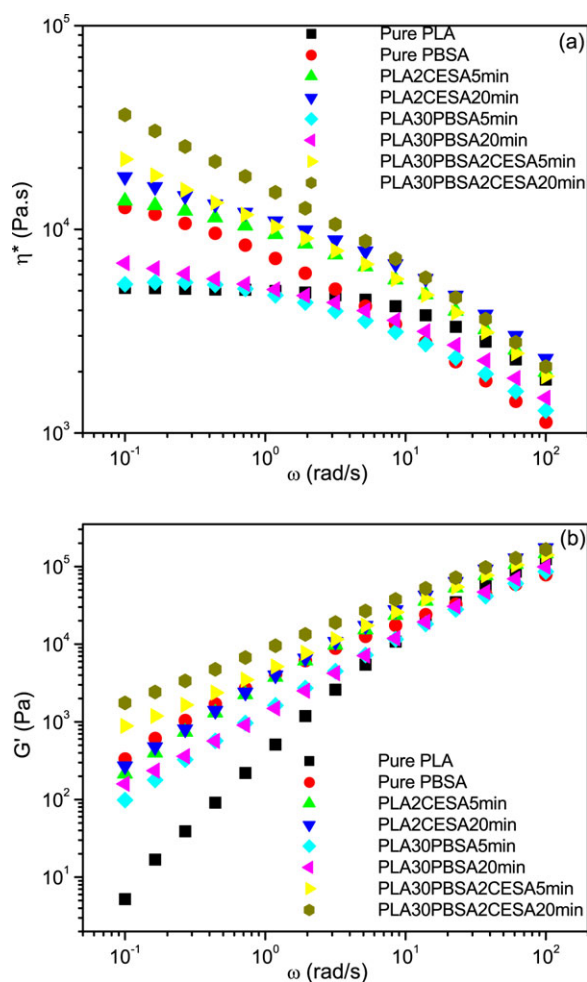


**Figure 10.** Linear viscoelastic properties of the PLA/PBSA blends: (a)  $\eta^*$  and (b)  $G'$ . [Color figure can be viewed in the online issue, which is available at [wileyonlinelibrary.com](http://wileyonlinelibrary.com).]



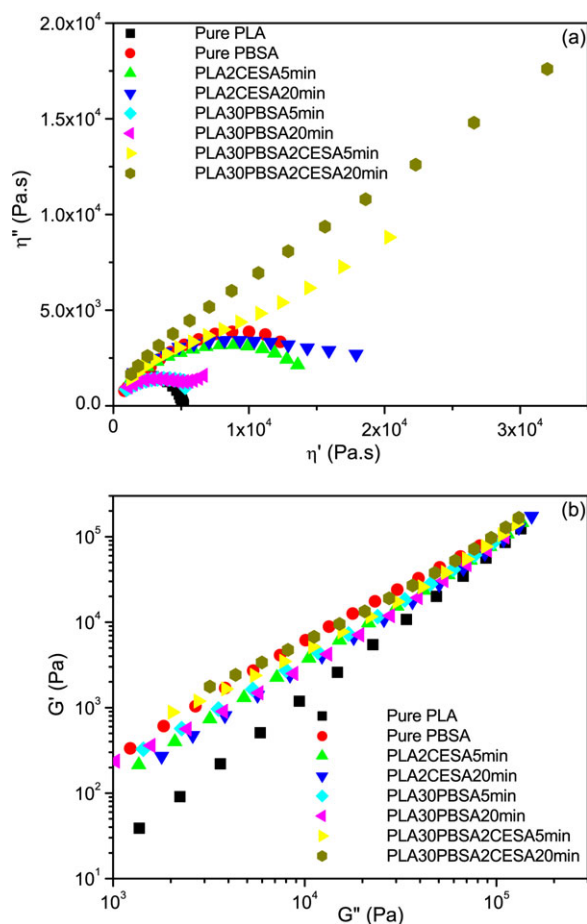


**Figure 11.** Cole–Cole plot of the PLA/PBSA blends with and without chain extender at various mixing times: (a) Cole–Cole plot and (b) modified Cole–Cole plot. [Color figure can be viewed in the online issue, which is available at [wileyonlinelibrary.com](http://wileyonlinelibrary.com).]

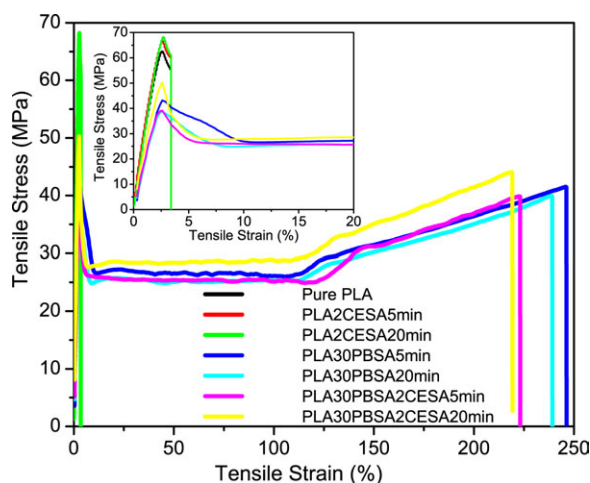


**Figure 12.** Stress–strain curve of the PLA/PBSA blends with and without chain extender. [Color figure can be viewed in the online issue, which is available at [wileyonlinelibrary.com](http://wileyonlinelibrary.com).]

and PLA with chain extender, are plotted in Figures 14 and 15. Figure 14(a,b) shows the results for compounds prepared with a 5-min mixing time, and Figure 15(a,b) shows the results for compounds prepared with the 20-min mixing time. The results reveal that the elastic moduli of the blends (with and without chain extender) were lower than those of the pure PLA and PLA with chain extender. However, the elastic moduli of all of the compounds were higher than that of pure PBSA. The strain at break, on the other hand, increased with the incorporation of PBSA. A dramatic increase in the elongation at break of the blends suggests good adhesion between the blend components. To visualize the adhesion between the blend components, the cross sections of the samples after tensile testing were examined with the electron microscope. Figure 16 shows FE-SEM images of the PLA/PBSA blends with chain extender at two different magnifications. The figure shows no clear sign of debonding in the ruptured samples; this indicates that there was good adhesion between the components. Interestingly, neither the chain extender nor the mixing time had a significant influence on the modulus or strain at break of the PLA/PBSA blends. In other words, the elastic modulus and elongation at break of the blends with and without chain extender were almost the same, regardless of the mixing time. However, the results of the rheological measurements (reported in the previous section) show

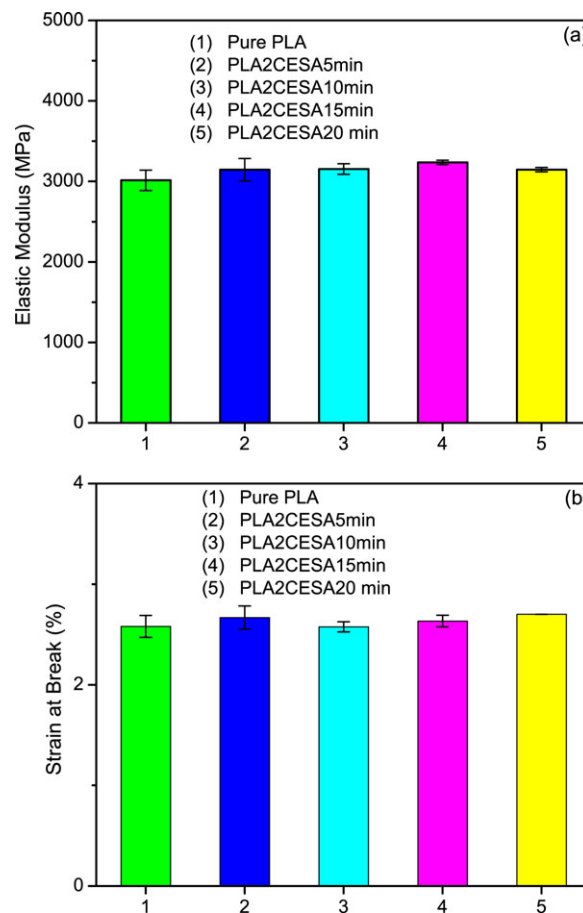


**Figure 13.** Mechanical properties of PLA with chain extender: (a) elastic modulus and (b) strain at break. [Color figure can be viewed in the online issue, which is available at [wileyonlinelibrary.com](http://wileyonlinelibrary.com).]

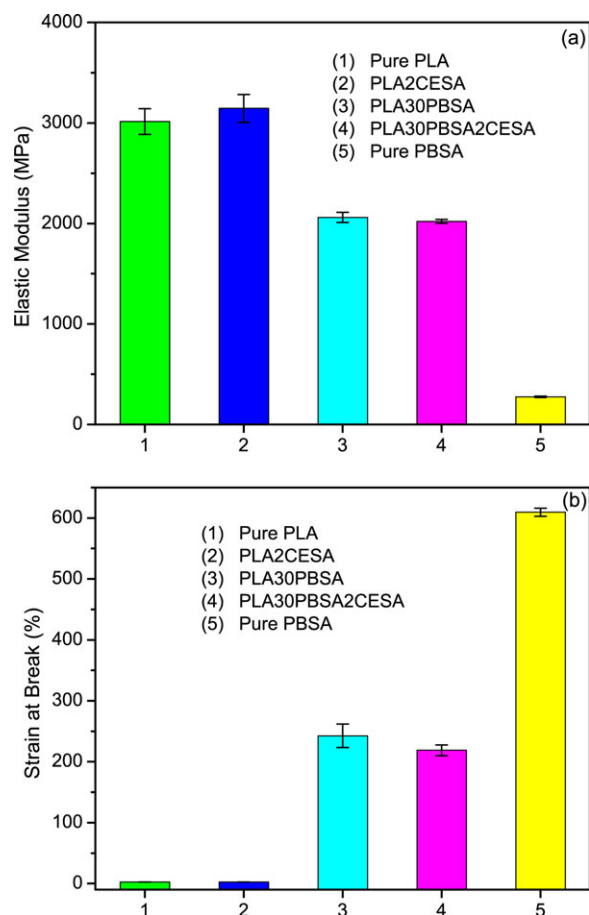


**Figure 14.** Mechanical properties of the PLA/PBSA blends with and without chain extender (mixing time = 5 min): (a) elastic modulus and (b) strain at break. [Color figure can be viewed in the online issue, which is available at [wileyonlinelibrary.com](http://wileyonlinelibrary.com).]

that the chain extender improved the melt strength of the PLA/PBSA blends considerably. Therefore, the mixing of PLA with PBSA in the presence of chain extender imparted melt strength to the blends with high ductility.

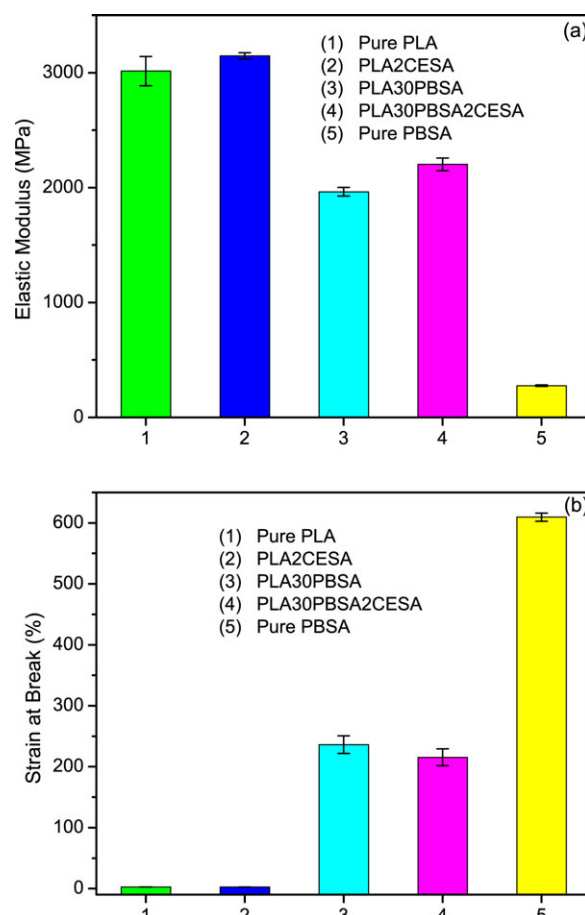


**Figure 15.** Mechanical properties of the PLA/PBSA blends with and without chain extender (mixing time = 20 min): (a) elastic modulus and (b) strain at break. [Color figure can be viewed in the online issue, which is available at [wileyonlinelibrary.com](http://wileyonlinelibrary.com).]

## CONCLUSIONS

The use of a chain extender imparted strain-hardening behavior to the PLA melts. This effect became stronger as the mixing time increased. The blends containing chain extender exhibited

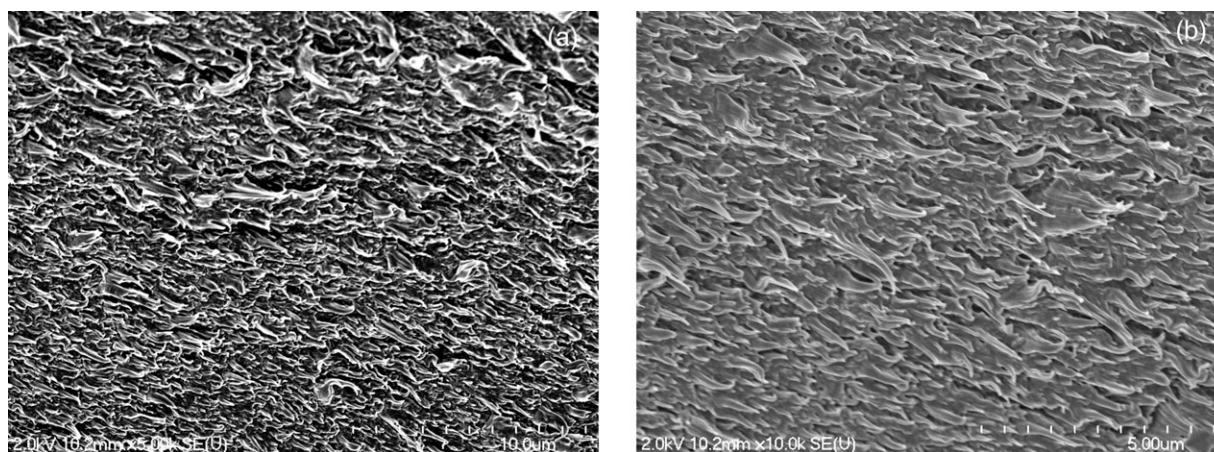


**Figure 16.** Cross-sectional FE-SEM images of the PLA/PBSA/CESA blends (mixing time = 20 min) after tensile testing at two different magnifications.

strong melt strain-hardening behavior, whereas the blends without chain extender exhibited weak strain-hardening behavior. The results of the linear viscoelastic measurements suggested that chain branching occurred in compounds with chain extender. The chain-branched structure was likely responsible for the rheological effects, such as the high  $G'$  and  $\eta^*$  at low  $\omega$ , increased shear sensitivity, long relaxation time, and strong strain-hardening behavior, observed for the blends with chain extender. The results of tensile testing showed that PBSA significantly enhanced the ductility of the PLA/PBSA blends. Interestingly, the chain extender had no significant effect on the modulus and elongation at break of the blends. Therefore, the blending of PLA with PBSA in the presence of chain extender imparted melt strength to the blends with high ductility. We concluded that the strategy of combining blending with the chain-extension reaction enhanced both the ductility and melt strength of the PLA systems and helped us to render them more suitable for many end-use applications.

#### ACKNOWLEDGMENTS

One of the authors (H.E.) is grateful to the government of Quebec for the two-year postdoctoral fellowship award from the Fonds Québécois de la Recherche sur la Nature et les Technologies. The authors acknowledge financial support provided by the Natural Sciences and Engineering Research Council of Canada. The authors are also grateful to Clariant Masterbatches for kindly providing the chain extender used in this study.

#### REFERENCES

1. Lim, L. T.; Auras, R.; Rubino, M. *Prog. Polym. Sci.* **2008**, *33*, 820.
2. Jiang, L.; Wolcott, M. P.; Zhang, J. *Biomacromolecules* **2005**, *7*, 199.
3. Eslami, H.; Kamal, M. *J. Appl. Polym. Sci.* **2013**, *127*, 2290.
4. Eslami, H.; Kamal, M. 70th Annual Technical Conference of the Society of Plastics Engineers 2012 (ANTEC 2012); Society of Plastics Engineers: Orlando, **2012**; p 155.
5. Corre, Y.-M.; Duchet, J.; Reignier, J.; Maazouz, A. *Rheol. Acta* **2011**, *50*, 613.
6. Li, H.; Huneault, M. A. *J. Appl. Polym. Sci.* **2011**, *122*, 134.
7. Mihai, M.; Huneault, M. A.; Favis, B. D. *Polym. Eng. Sci.* **2010**, *50*, 629.
8. Lee, S.; Lee, J. W. *Korea–Aust. Rheol. J.* **2005**, *17*, 71.
9. Li, K.; Peng, J.; Turng, L.-S.; Huang, H.-X. *Adv. Polym. Technol.* **2011**, *30*, 150.
10. Wang, Y.; Mano, J. F. *J. Appl. Polym. Sci.* **2007**, *105*, 3204.
11. Yeh, J. T.; Tsou, C. H.; Huang, C. Y.; Chen, K. N.; Wu, C. S.; Chai, W. L. *J. Appl. Polym. Sci.* **2010**, *116*, 680.
12. Zhang, N.; Wang, Q.; Ren, J.; Wang, L. *J. Mater. Sci.* **2009**, *44*, 250.
13. Ko, S. W.; Gupta, R. K.; Bhattacharya, S. N.; Choi, H. *J. Macromol. Mater. Eng.* **2010**, *295*, 320.
14. Ray, S. S.; Bousmina, M. *Polymer* **2005**, *46*, 12430.
15. Sentmanat, M.; Wang, B. N.; McKinley, G. H. *J. Rheol.* **2005**, *49*, 585.
16. Sentmanat, M. L. *Rheol. Acta* **2004**, *43*, 657.
17. Cao, K.; Li, Y.; Lu, Z.-Q.; Wu, S.-L.; Chen, Z.-H.; Yao, Z.; Huang, Z.-M. *J. Appl. Polym. Sci.* **2011**, *121*, 3384.
18. Tian, J.; Yu, W.; Zhou, C. *Polymer* **2006**, *47*, 7962.
19. Dae Han, C.; Kim, J. K. *Polymer* **1993**, *34*, 2533.
20. Kim, J. Y.; Park, H. S.; Kim, S. H. *J. Appl. Polym. Sci.* **2007**, *103*, 1450.
21. Kwag, H.; Rana, D.; Cho, K.; Rhee, J.; Woo, T.; Lee, B. H.; Choe, S. *Polym. Eng. Sci.* **2000**, *40*, 1672.